

---

# Radial Endoscopic Ultrasound

---

*Scott T. Cooper, MD  
and Michael K. Sanders, MD*

## **CONTENTS**

INTRODUCTION  
EQUIPMENT  
GASTROINTESTINAL TRACT WALL  
MEDIASTINUM AND ESOPHAGUS  
STOMACH  
PANCREAS AND EXTRAHEPATIC BILE DUCT  
RECTUM  
SUMMARY

---

### *Abstract*

Over the past decade, radial endoscopic ultrasonography has emerged as a powerful diagnostic tool for evaluating and staging neoplasms of the gastrointestinal tract. Although the initial radial echoendoscopes were heavy, cumbersome instruments, technological advances have resulted in slimmer, lighter scopes with increased agility and a wider range of ultrasound frequencies. Initially, this technology was limited to large, tertiary referral centers due to excessive equipment costs and lack of skilled endosonographers. However, the ever increasing demand for EUS has led to investment in both equipment and experienced endosonographers by some smaller community programs and private practitioners. For the beginner, understanding the basic principles of radial EUS is fundamental for

From: *Clinical Gastroenterology: Endoscopic Ultrasound*,  
Edited by: V. M. Shami and M. Kahaleh, DOI 10.1007/978-1-60327-480-7\_3,  
© Springer Science+Business Media, LLC 2010

establishing the skill set necessary to perform an accurate and efficient exam. A systematic approach to each anatomical station of the digestive tract is critical for assuring a thorough and complete exam. Review of both anatomical and radiologic atlases is helpful for the beginner to understand and accurately interpret ultrasound images. This chapter focuses on the technical details of performing radial EUS on the upper gastrointestinal tract and rectum. Furthermore, attention is directed toward the recognition of common anatomical landmarks in efforts to improve both the efficiency and accuracy of the exam. Although reading a textbook chapter obviously does not substitute for dedicated, supervised hands-on training, a general understanding of the procedure and common anatomical landmarks is crucial to begin EUS training.

**Key Words:** Endosonography, Radial EUS, EUS stations

## INTRODUCTION

Radial endosonography provides a high-resolution, 360° circumferential imaging of the gastrointestinal tract and its surrounding structures. The images created are in a plane perpendicular to the axis of the tip of the endoscope. Therefore, when orienting the echoendoscope along the long axis of the body, images obtained are comparable to those generated with conventional computed tomography (CT) scans. The images produced by the newer radial echoendoscopes rival or surpass other imaging techniques such as magnetic resonance imaging (MRI), CT scans, and transcutaneous ultrasound (1–4). The main disadvantage of radial echoendoscopes, in contrast to linear echoendoscopes, is their inability to allow directed fine needle aspiration or other therapeutic interventions. However, radial endosonography has developed into an invaluable tool for the diagnosis and staging of gastrointestinal neoplasms in the upper gastrointestinal tract and rectum.

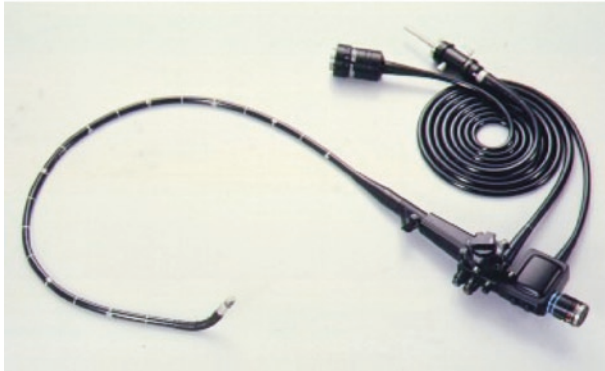
This chapter provides a brief introduction to available radial echoendoscopes as well as some basic principles for radial imaging of the normal upper gastrointestinal tract and rectum. Since the indications for radial EUS are covered in the subsequent chapters, we focus on performing the exam and recognizing common anatomical landmarks. In addition, we have supplied additional references that may provide useful information for the beginner in endosonography (5–7).

## EQUIPMENT

Initially, radial echoendoscopes were manufactured with a heavy motor housed in the endoscope handle. The motor drove an ultrasound transducer, which was immersed in an oil bath, located at the tip of the endoscope beyond an oblique-viewing lens. The ultrasound frequencies were limited to 7.5 and 12 MHz. Figure 1 depicts two early fiberoptic echoendoscopes produced by Olympus (Olympus America Inc, Center Valley, PA), which for many years were the standard instruments for endosonography. Later, the motor was incorporated into the umbilical cord connecting the endoscope to the endoscopic processor. In addition, the oil bath was made smaller. These modifications provided the endosonographer with a lighter, slimmer echoendoscope with improved agility and wider range of frequencies (5, 7.5, 12, and 20 MHz) (Fig. 2).



Olympus GF-UM2



Olympus GF-UM20

**Fig. 1.** GF-UM2 (1984) and GF-UM20 (1991) are two fiberoptic echoendoscopes produced by Olympus (Olympus America Inc, Center Valley, PA). The motor was housed in the handle of the endoscope making these instruments heavier and more cumbersome for the endoscopist. Frequencies were limited to 7.5 and 12 MHz (Photos courtesy of Olympus, Inc.).

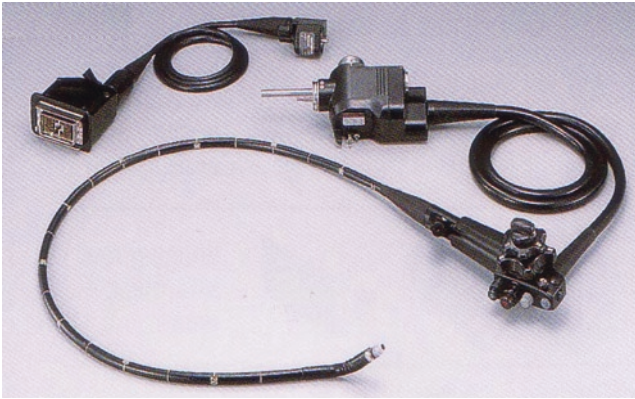


**Fig. 2.** Olympus GF-UM160 model transferred the motor into the umbilicus providing a light weight instrument with increased agility and wider range of ultrasound frequencies (5, 7.5, 12, and 20 Hz) (Photo courtesy of Olympus, Inc).

More recently, electronic radial echoendoscopes that house an electronic ultrasound transducer immediately beyond an oblique-viewing lens at the tip of the endoscope have been manufactured (Fig. 3). Some feel that electronic radial transducers are less prone to breakage as they lack the mechanical drive shaft and oil bath of mechanical echoendoscopes. Moreover, electronic radial echoendoscopes have the benefit of providing real-time detection of flow (color Doppler), thereby allowing the differentiation between arterial and venous blood flow with pulse Doppler.

For both mechanical and electronic radial echoendoscopes, acoustic coupling between the ultrasound probe and structure of interest is obtained by instilling water into a balloon covering the circumference of the ultrasound probe (Fig. 4). The balloon can be inflated and deflated by valves on the endoscope handle. Once inflated with water, it is extremely important to remove any remaining air bubbles from the balloon to avoid artifact imaging. Acoustic coupling can be further enhanced during the exam by instilling water into the intestinal lumen through the biopsy channel.

For many years, mechanical radial echoendoscopes produced by Olympus were the standard equipment for endosonographers. Pentax (Pentax of America, Montvale, NJ) was the first company to release an electronic radial echoendoscope. Today, there are three leading manufacturers of radial echoendoscopes: Olympus, Pentax, and Fujinon (Fujinon USA Inc, Wayne, NJ). Table 1 lists some of the technical specifications of commonly used radial echoendoscopes (8). For a discussion on ultrasound processors, please refer to the preceding chapter on endosonographic instrumentation.



GF-UE160AL

**Fig. 3.** Olympus GF-UE160AL has an electronic ultrasound transducer located beyond the oblique-viewing lens. The GF-UE160AL is compatible with the Aloka processor, traditionally used for linear endosonography (Photos courtesy of Olympus, Inc).



**Fig. 4.** A balloon covers the circumference of the ultrasound probe and can be inflated with water to enhance acoustic coupling.

**Table 1**  
**Technical specifications of commonly available radial echoendoscopes**

<i>Manufacturer</i>	<i>Pentax</i>	<i>Olympus</i>	<i>Olympus</i>	<i>Olympus</i>	<i>Olympus</i>	<i>Olympus</i>
Model	EG-3630UR	GF UM20	GF UM130	GF UMQ130	GF UM160	GF-UE 160-ALS
Imaging	Video	Fiberoptic	Video	Video	Video	Video
Transducer	Electronic	Mechanical	Mechanical	Mechanical	Mechanical	Electronic
Specifications						
Working length	1,250	1,055	1,250	1,250	1,250	1,250
Insertion tube diameter (mm)	12.1	13.2	12.7	12.7	12.7	11.8
Working channel diameter (mm)	2.4	2	2.2	2.2	2.2	2.2
Tip deflection,	130–60	130	130	130	130	90–130
up-down (degree)						
Tip deflection	60–60	90	90	90	90	90
right-left (degrees)						
Direction of viewing field	Forward	45 forward	50 forward	50 forward	50 forward	55 forward
(degrees)		oblique	oblique	oblique	oblique	oblique
Field of view (degree)	120	80	100	100	100	100
Depth of field (mm)	30–150	3–100	3–100	3–100	3–100	3–100
Acoustic frequency (MHz)	5/7.5/10	7.5/12	7.5/12	7.5/20	5/7.5/12/20	5/6/7.5/10
Scanning angle (degree)	270	360	360	360	360	360

## GASTROINTESTINAL TRACT WALL

Unlike other radiographic imaging modalities, endoscopic ultrasound provides superior, detailed imaging of the gastrointestinal wall with five distinct sonographic layers corresponding to their histologic structures (Fig. 5). Previous studies have confirmed the histologic correlates of gastrointestinal ultrasound images (9, 10).

The layer closest to the lumen of the gastrointestinal tract appears as a bright (hyperechoic) structure, which corresponds to the interface between the mucosa and the ultrasound transducer or its surrounding fluid. The second layer of the gastrointestinal tract is a dark (hypoechoic) layer that represents the deep mucosa, or muscularis mucosa. The third sonographic layer corresponds to the submucosa (hyperechoic) and is caused by the acoustic interface between the submucosa

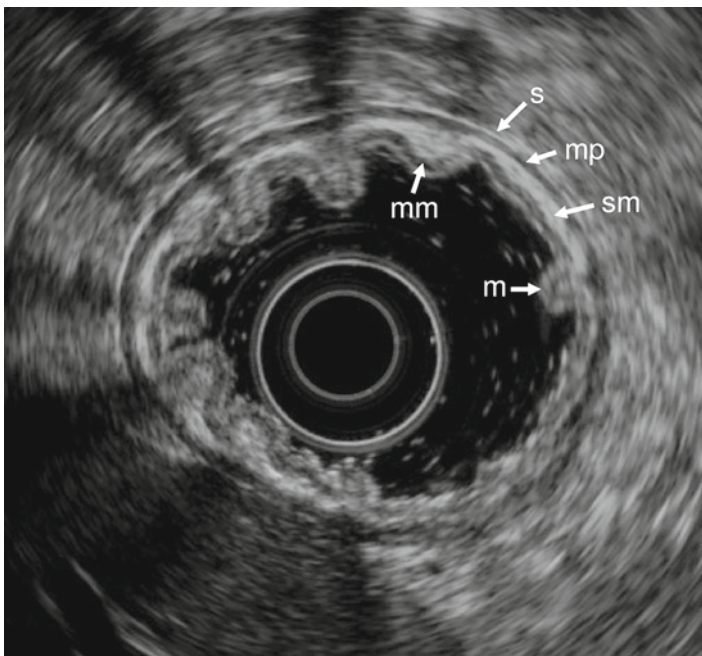


**Fig. 5.** Ultrasound image of the gastric wall demonstrating five distinct sonographic layers. The superficial mucosa (m) is hyperechoic and represents the first layer. The second layer is the hypoechoic, deep mucosa, or muscularis mucosa (mm). The submucosa (sm) is hyperechoic and corresponds to third layer. The fourth layer, muscularis propria (mp) is hypoechoic. The serosa (s) is the fifth layer and hyperechoic.



and denser muscularis propria. The muscularis propria is hypoechoic and corresponds to the fourth sonographic layer. In some areas of the digestive tract, the fourth layer (muscularis propria) is divided by a thin bright, hyperechoic layer caused by the separation of the inner circular and outer longitudinal muscle layers of the muscularis propria. In these regions, the intestinal wall may demonstrate a seven layer pattern. The last, and deepest, sonographic layer is a bright, hyperechoic structure that corresponds to the serosa in the stomach and small bowel and adventitia in the esophagus. At higher ultrasound frequencies (20–30 MHz), separation of the muscularis mucosa and muscularis propria into the inner circular and outer longitudinal muscle layers may be appreciated, thereby demonstrating a nine layer pattern to the gastrointestinal tract wall (11). Understanding the correlation between the sonographic layers and histologic structures is critical for the diagnosis of subepithelial lesions and staging of gastrointestinal neoplasms.

## MEDIASTINUM AND ESOPHAGUS

The previously mentioned five sonographic layers of the gastrointestinal tract wall are easily demonstrated in the esophagus, which is typically about 3 mm thick. Due to its orientation parallel to the long axis of the body, images produced by radial EUS in the esophagus correlate nicely with transverse sections from thoracic CT scans. For the beginner, review of a radiology and/or anatomy atlas can be extremely helpful for interpreting EUS images of the mediastinum.

In order to avoid confusion for the beginner, unless otherwise specified, when describing the anatomical stations for radial EUS, “right” will refer to the patient’s right and “left” will refer to the patient’s left. As with CT imaging, the location of the anatomical structures on the monitor screen is often opposite of the anatomic location.

### *Distal Esophagus*

As with all EUS examinations, a systematic approach should be applied to examine the esophagus and mediastinum, paying close attention to anatomical landmarks for proper orientation. For imaging the upper gastrointestinal tract, generally we begin with a frequency setting between 5 and 7.5 MHz and a range between 6 and 9 cm. These settings provide a general overall view of the anatomy and can be adjusted depending on the lesion of interest. The esophageal exam should begin at the gastroesophageal junction and progress proximally. The balloon



should be inflated to disperse any intraluminal air, and the transducer should be centered in the balloon. One must be careful to avoid overinflation of the balloon as this may compress the esophageal wall and interfere with either detection or staging of neoplasms. The aorta is a constant landmark throughout the exam until withdrawal above the aortic arch. The aorta is seen as a large anechoic structure with hyperechoic walls and measures ~1.5–2 cm in diameter. Maintaining the aorta in the 5–6 o'clock position will simulate anatomical findings observed on transverse CT sections of the mediastinum. As the esophagus is a straight, tubular structure, little manipulation of the ultrasound probe is necessary to maintain proper image orientation.

While maintaining the aorta in the 5 o'clock position, the spine is observed in the 7 o'clock position. Due to its dense nature and poor ultrasound wave penetration, the spine produces an irregular hyperechoic image with significant acoustic artifact. At the 6–12 o'clock position the liver can be seen. In the liver parenchyma, the hepatic veins and intrahepatic bile ducts can be appreciated as completely black (anechoic) structures (Fig. 6). In the distal esophagus, the fundus of the stomach is found in the 1–4 o'clock position (Fig. 7). The stomach can be easily identified by the rugal folds.

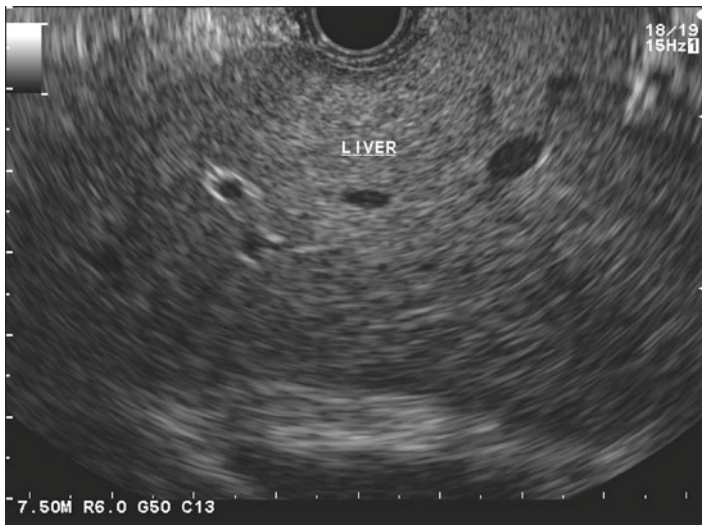


**Fig. 6.** Left lobe of the liver. The completely black (anechoic) structures within the liver parenchyma represent the hepatic veins and intrahepatic bile ducts.

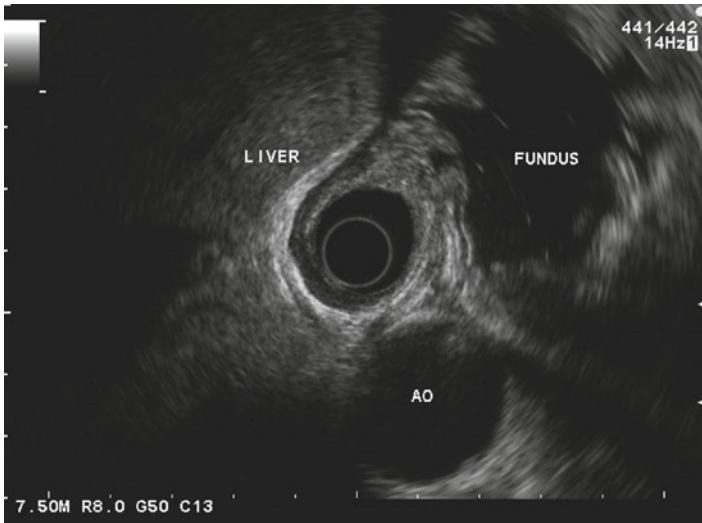


**Fig. 7.** Imaging of the distal esophagus reveals the fundus, liver, and aorta (AO).

### *Midesophagus*

As the radial echoendoscope is withdrawn to the midesophagus, the left atrium emerges into the 12 o'clock position (Fig. 8). Often, the mitral valve can be visualized as well. The right and left lungs can be seen at the 9 and 2 o'clock positions, respectively, as hyperechoic rings. The azygous vein appears as a hypoechoic structure to the right of the aorta and eventually courses anterior to the spine toward the right lung as the echoendoscope is withdrawn (Fig. 8). The left and right main stem bronchi are seen as hyperechoic rings at the 1 and 11 o'clock positions, respectively, and merge to form the trachea, found in the 12 o'clock position. Significant air artifact is produced by the bronchi and trachea. The inferior tracheobronchial, or carinal lymph nodes are seen at this level, often in the subcarinal space. Normal lymph nodes are seen as hypoechoic, heterogeneous structures with internal hyperechoic foci and poorly defined nodal margins. Benign lymph nodes may also appear to "drape" across the ultrasound transducer in this region. As the echoendoscope is withdrawn further, the arch of the aorta can be seen to the left of the descending aorta (Fig. 9). The aortapulmonary window (APW) can be examined in this region with slight scope tip deflection into the aortic arch and gentle advancement and withdrawal of the echoendoscope (Fig. 10). The APW is an important landmark for nodal staging in upper gastrointestinal malignancies. In the midesophagus, the thoracic duct can also be observed as a small, hypoechoic structure between the aorta and spine (Fig. 11).

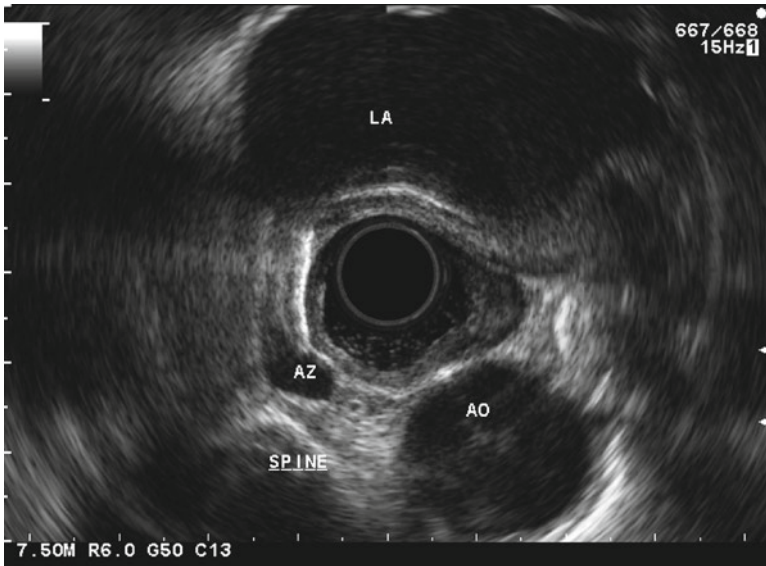


**Fig. 8.** Views of the midesophagus demonstrating the aorta (AO), left atrium (LA), azygous vein (AZ), and spine.

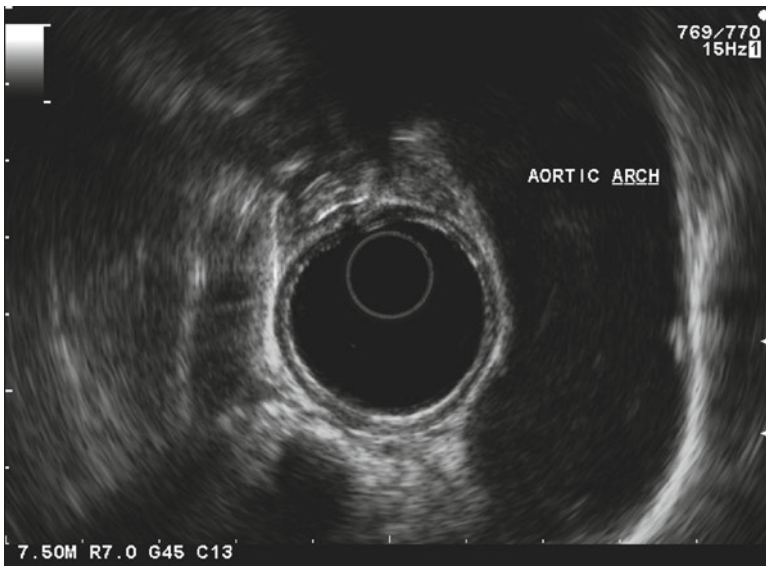


**Fig. 9.** The aortic arch can be appreciated upon withdrawal from the mid-proximal esophagus.

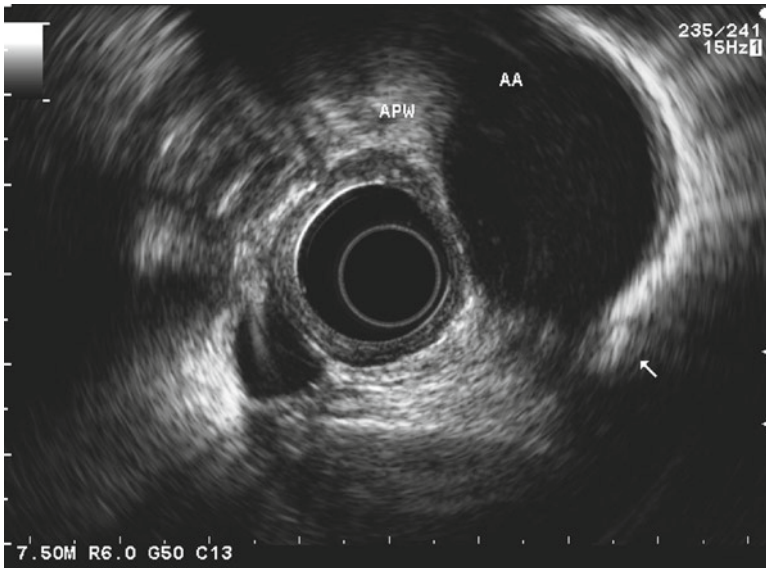


**Fig. 10.** The aortopulmonary window (APW) is observed at the level of the aortic arch and represents an important landmark for nodal staging.

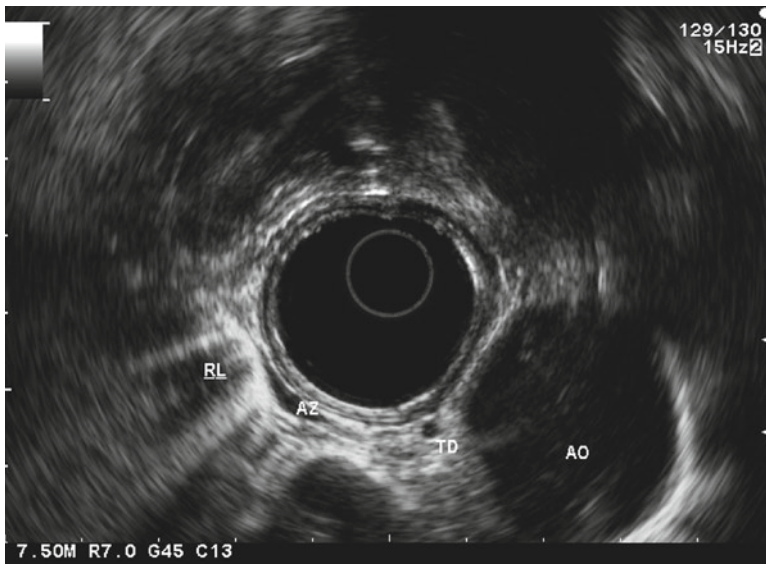


**Fig. 11.** The thoracic duct (TD) can be observed between the aorta and spine in the midesophagus. The azygous vein (AZ) and right lung (RL) are also demonstrated.

### *Proximal Esophagus*

Just proximal to the aortic arch, one can visualize the left common carotid artery at the 1–2 o'clock position and the left subclavian artery at the 2 o'clock position. As the echoendoscope is withdrawn further, just distal to the upper esophageal sphincter, one can image the thyroid gland, a hyperechoic structure, at the 11 and 1 o'clock position on either side of the trachea, which is seen just to the left of the 12 o'clock position. The thymus can sometimes be visualized just distal to the thyroid.

At this level, one can also image the left and right internal jugular veins located at the 3 and 8 o'clock position, respectively. The left and right carotid arteries are seen just beside and medial to the left and right internal jugular veins. For practical purposes, this region does not contain any significant anatomical landmarks; however, it is extremely important for determining the presence or absence of periesophageal and/or paratracheal lymph nodes when staging upper gastrointestinal malignancies.

## STOMACH

Similar to the esophageal exam, examination of the stomach typically begins distally in the prepyloric antrum. The balloon is fully inflated and continuous suction is applied to remove any air from the gastric lumen. Once the gastric wall is collapsed, the echoendoscope is slowly withdrawn to the level of the fundus, paying close attention to both the gastric wall and perigastric structures. Once an abnormality is observed, specific techniques are applied to acquire more detailed imaging.

The five layers of the gastric wall can be easily identified, and typically the wall measures between 3 and 5 mm in diameter. In some regions of the stomach, it may be difficult to achieve perpendicular, high-quality imaging of the gastric wall. This becomes particularly difficult in the antrum, and it may be impossible to adjust either the scope position or tip deflection for adequate imaging. In these circumstances, either a radial miniprobe or instillation of water (100–300 ml) may be necessary to either provide better positioning or enhance acoustic coupling for an adequate exam. When instilling water, the examiner must be aware of the potential aspiration risk and therefore work quickly and efficiently to complete the exam.

When the echoendoscope tip is positioned in the antrum, the anterior wall of the stomach is seen on the left of the ultrasound image and the posterior wall is observed on the right. The gallbladder, which has



three sonographic layers, can be easily imaged from the antrum (Fig. 12). Often times stones, which appear as hyperechoic structures with posterior shadowing (Fig. 13), or sludge, hyperechoic material that lies in the dependent portion of the gallbladder, can be seen. The head and genu of the pancreas along with its surrounding vasculature can also be seen from the antrum.

Withdrawing the echoendoscope into the midbody of the stomach allows visualization of the pancreatic body (Fig. 14). Examination of the pancreas is discussed in further detail in the following section. The splenic hilum, splenic artery and vein, left kidney, portions of the right lobe of the liver, and the entire left lobe of the liver can also be visualized from the stomach. A normal spleen generally has a homogeneous echotexture that is similar to or slightly brighter than the density of the liver. The left kidney contains multiple rings with hyperechoic borders corresponding to the renal calyces (Fig. 15).

When the echoendoscope is positioned immediately below the gastroesophageal junction, the celiac trunk can be seen branching off into the splenic and common hepatic arteries (Fig. 16). Once the celiac axis has been identified, slight withdrawal and clockwise rotation will bring the left adrenal gland into view between the aorta and left kidney

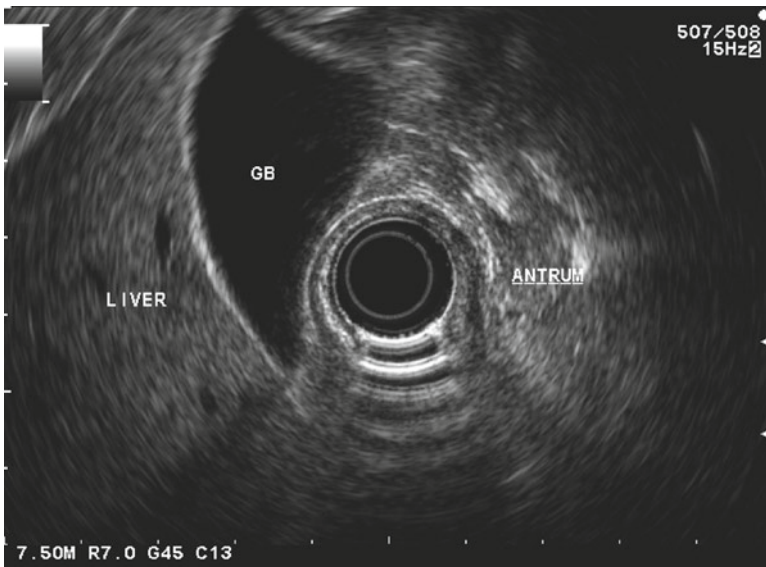


**Fig. 12.** Ultrasound image from the prepyloric antrum demonstrating the gallbladder (GB) and liver.

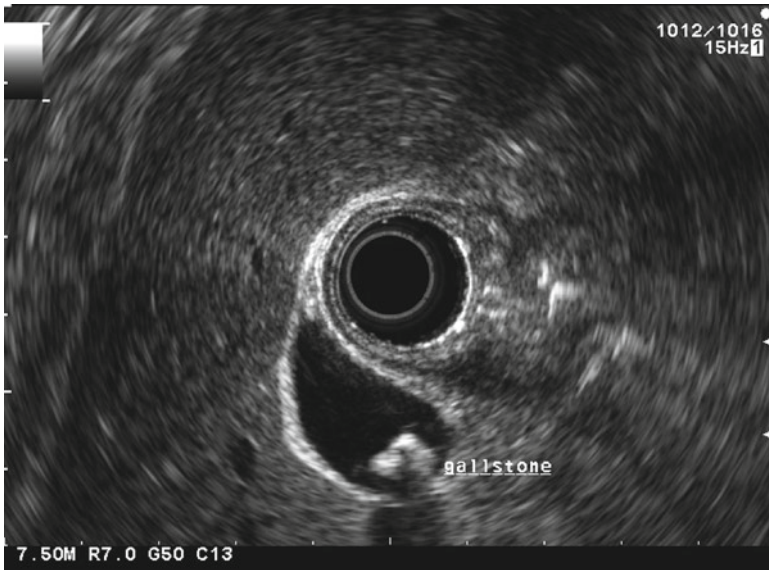


**Fig. 13.** Gallbladder with hyperechoic gallstones (GS).

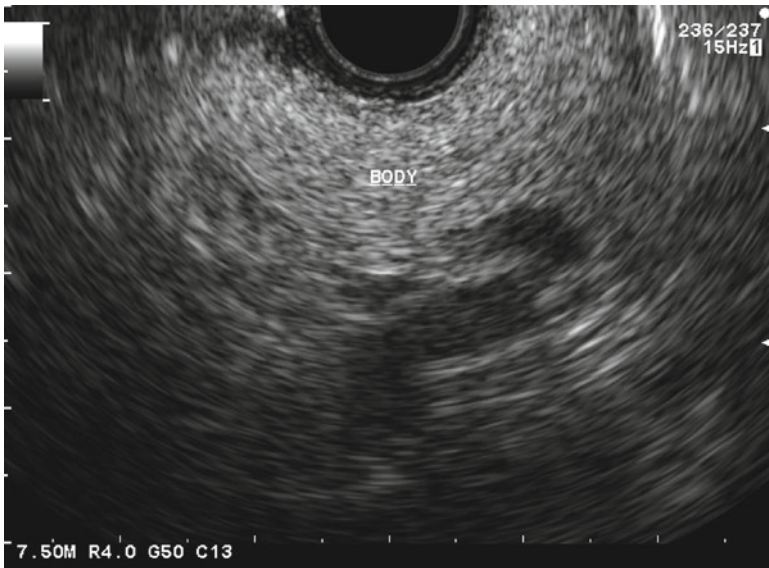


**Fig. 14.** Body of the pancreas can be seen from the midbody of the stomach. The normal parenchyma displays a fine, speckled pattern often described as having a “salt and pepper” appearance.



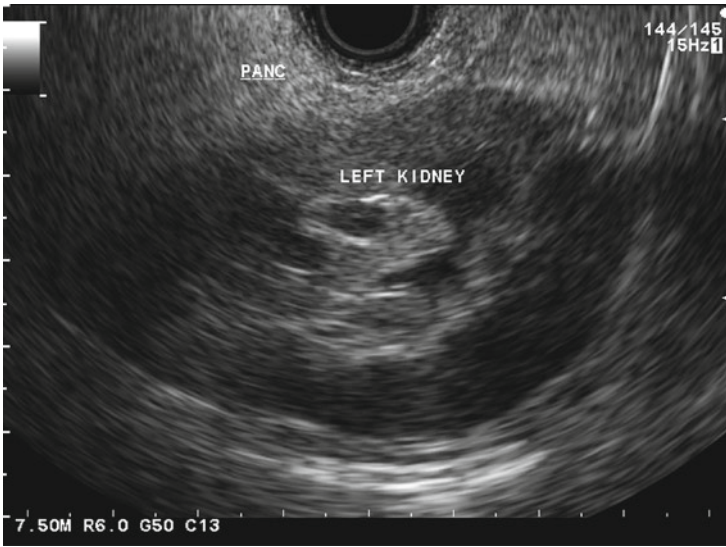


**Fig. 15.** The left kidney is easily recognizable from the midbody of the stomach. Often times, the pancreatic body (PANC) can be found between the left kidney and ultrasound transducer.

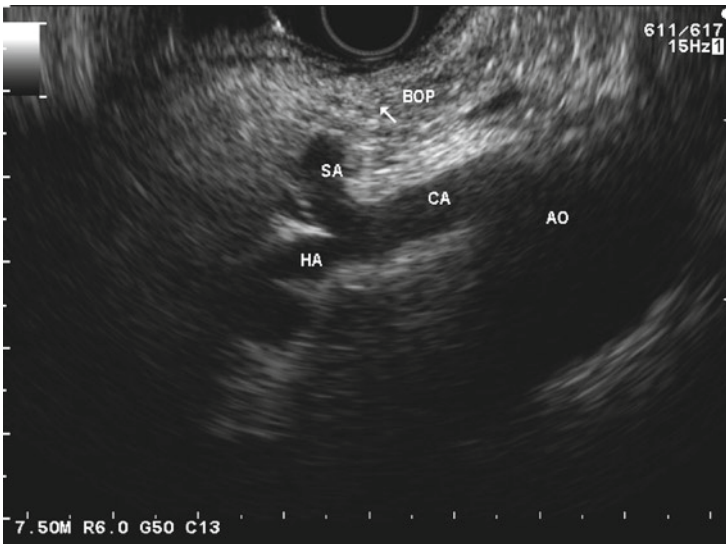


**Fig. 16.** The celiac artery (CA) arising from the aorta (AO) and bifurcating into the splenic (SA) and common hepatic arteries (HA) observed immediately below the gastroesophageal junction. The splenic artery also serves as a useful landmark for locating the body of the pancreas (BOP).

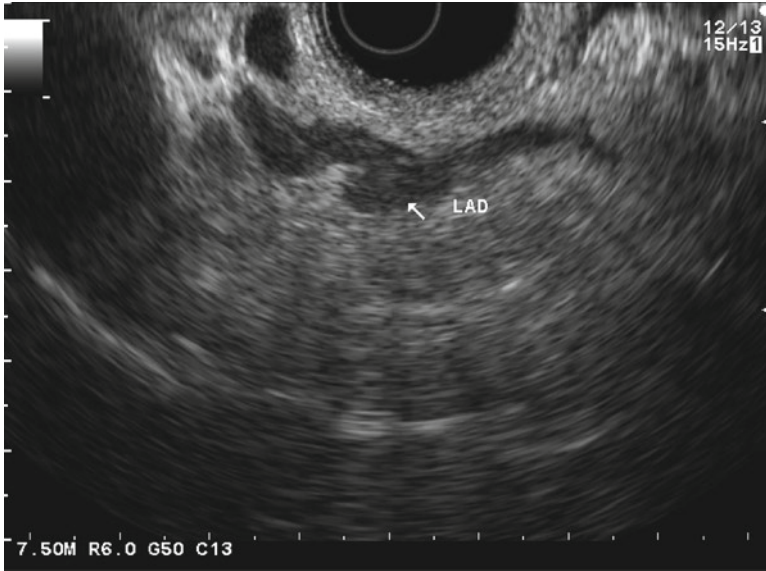


**Fig. 17.** The left adrenal gland (LAD) is located between the aorta and left kidney. One can appreciate its likening to a “seagull” with outstretched wings.

(Fig. 17). The adrenal gland has been described as a “seagull” with its outstretched wings.

The beginner should quickly become familiar with these important anatomical landmarks as the stomach is large and easily distended, making it simple to become disoriented. Quick recognition of these landmarks will improve both the efficiency and accuracy of your exam.

## PANCREAS AND EXTRAHEPATIC BILE DUCT

The pancreas is imaged from both the body of the stomach and duodenum. A normal pancreas has a homogenous, fine speckled pattern that is often described as having a “salt and pepper” appearance (Fig. 14). The border of a normal pancreas is generally smooth. With the echoendoscope, the main pancreatic duct can be traced from the pancreatic head to the tail. As a general rule, the normal pancreatic duct measures between 3 and 4 mm in diameter in the head and tapers to 2 mm in the body and 1 mm in the tail. Usually, the wall of the pancreatic duct is barely perceivable. Side branches may be appreciated

within the pancreatic head. The dorsal pancreas is generally more echogenic than the ventral pancreas. This is thought to be secondary to the higher fat content of the dorsal pancreas. In up to 75% of patients, the ventral anlage which represents the transition zone between the dorsal and ventral pancreas can be seen on EUS (12) (Fig. 18).

Similar to the esophagus and stomach, it is best to begin with a systematic approach when imaging the pancreas. The body and tail can be examined through the posterior wall of the stomach, whereas imaging of the head requires three separate positions within the duodenum: the apex of the duodenal bulb, immediately opposite the papilla, and just distal to the papilla for adequate imaging of the uncinata. Typically, we begin with imaging of the head from the duodenal bulb. Once the echoendoscope is advanced through the pylorus, the balloon is inflated, and the scope tip is deflected slightly downward with advancement of the echoendoscope into the apex. Typically, this maneuver will bring the head of the pancreas into the 6–8 o'clock position. However, if the examiner is having difficulty identifying the pancreatic head, the liver can serve as an excellent landmark from this position and is more easily identifiable. Once the liver is identified, the image should be rotated such that the

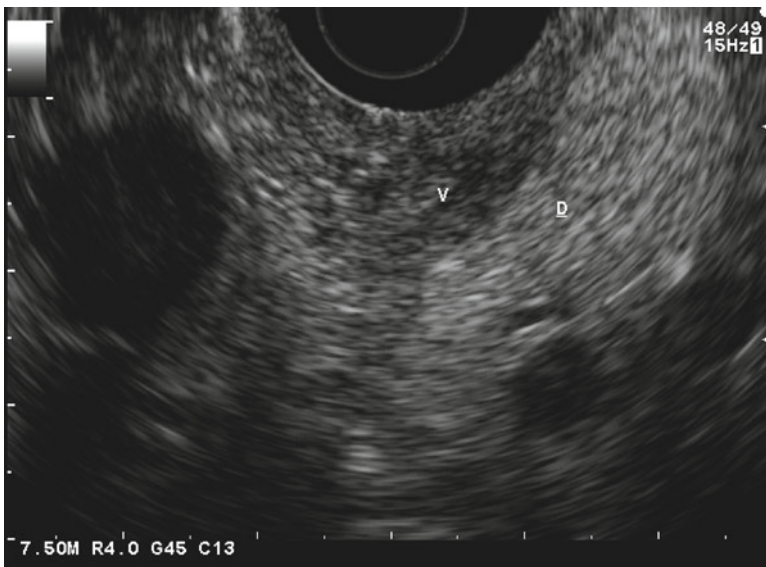


**Fig. 18.** Ventral anlage represents the transition between the hypoechoic ventral pancreas (V) and the more echogenic dorsal (D) pancreas. This image can be demonstrated best during withdrawal from the second portion of the duodenum.

liver is oriented in the 10 o'clock position. With gentle advancement and withdrawal of the echoendoscope coupled with either upward or downward tip deflection and/or clockwise and counterclockwise torquing, the landmarks in the region should become apparent.

The first landmark should be the common bile duct (CBD) which is a tubular anechoic structure that extends from the duodenal wall upward to the liver. The bile duct travels closest to the transducer and typically measures up to 6 mm in diameter. From this position, withdrawal of the echoendoscope coupled with counterclockwise rotation will allow imaging of the bile duct toward the hilum while gentle advancement and clockwise rotation will trace the bile duct downward to the papilla. The second landmark is the main pancreatic duct, which may be difficult to see in the same plane as the CBD. The pancreatic duct is a smaller tubular structure and may be difficult to visualize, requiring gentle advancement and rotation of the echoendoscope. The portal vein is the largest tubular structure in this region and is positioned furthest from the transducer. The simultaneous view of the bile duct, pancreatic duct and portal vein from the apex of the duodenal bulb has been termed the "stack sign." (13) (Fig. 19). Some authors have reported that the absence of a

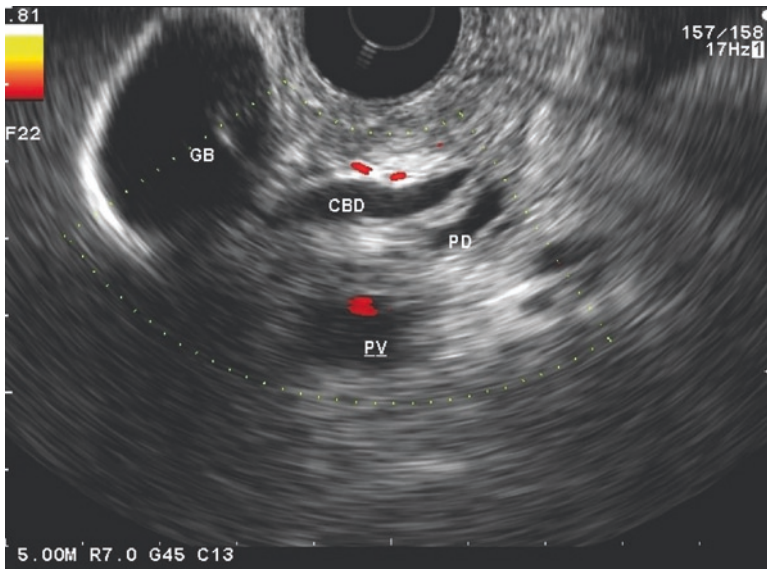


**Fig. 19.** Simultaneous view of the common bile duct (CBD), main pancreatic duct (PD), and portal vein (PV) from the apex of the duodenal bulb: the so-called stack sign. The gallbladder (GB) is also visualized.

“stack sign” may suggest the presence of pancreas divisum (14). Once the landmarks have been identified from the duodenal bulb, the echoendoscope is carefully advanced into the second portion of the duodenum. Since the radial echoendoscope is an oblique-viewing instrument, the examiner must be careful to avoid injury in this region as endoscopic visualization may be limited.

The second position for imaging the pancreatic head is from the level of the papilla. The papilla is best identified with direct endoscopic visualization followed by the placement of the ultrasound probe on top of the papilla. Balloon inflation followed by gentle advancement and withdrawal of the echoendoscope will allow imaging of the ampulla of Vater and pancreatic head. The bile duct and pancreatic duct can be seen in cross-section from this position with the pancreatic duct deep to the bile duct relative to the ultrasound transducer. This position is critical for accurate staging of ampullary neoplasms. In efforts to improve endosonographic imaging from this position, water may be instilled to enhance acoustic coupling and/or glucagon given to inhibit intestinal motility.

The third position required for a thorough, complete examination of the pancreatic head and uncinate region is located immediately distal to the major papilla. A major anatomical landmark in this region is the abdominal aorta. Once the echoendoscope is positioned beyond the papilla, withdrawal of the scope initially reveals the aorta in its longitudinal axis. Further withdrawal demonstrates the aorta in cross-section with the pancreas seen just to the right of the aorta on the monitor screen. The aorta should be oriented in the 7 o'clock position with the pancreas in the 6 o'clock position. From here, the echoendoscope is slowly withdrawn demonstrating the uncinate, ampulla, CBD, pancreatic duct, and ventral anlage (Fig. 18). As with routine upper endoscopy, a problem that may be encountered upon the withdrawal from the second portion of the duodenum is the tendency to fall back into the antrum. Similar to upper endoscopy, this problem may be avoided with slight withdrawal followed by slight advancement in attempts to maintain a one-to-one reaction with the shaft of the echoendoscope through this region. Despite this maneuver, adequate examination of this region may require several passes with the echoendoscope depending on the patient's anatomy.

After the head has been examined, attention is then focused on the body and tail. Generally, the body and tail are much easier to visualize, and the examination begins immediately below the gastroesophageal junction. The abdominal aorta is identified and oriented into the 6 o'clock position. The echoendoscope is advanced along the wall of the stomach to bring the first branch of the aorta, celiac artery, into view. If resistance is encountered upon advancing the echoendoscope, this



suggests the presence of a hiatal hernia and may require either tip deflection or scope rotation to avoid injury to the gastric wall. Once the bifurcation of the celiac artery is identified, the splenic artery can be traced to the pancreatic body (Fig. 16). Two major anatomical landmarks in this region are the splenoportal confluence and the splenic vein. The splenoportal confluence has been described as having a “club-like” appearance given its unique shape on radial imaging (Fig. 20). Once the splenoportal confluence and pancreatic body have been identified, the gland can be traced toward the genu with counter-clockwise torque and advancement of the scope or toward the tail with gentle withdrawal, clockwise rotation and some upward tip deflection. This produces an elongated view of the pancreas that can be easily traced back and forth with advancement and withdrawal of the echoendoscope. The splenic vein serves as a useful landmark for finding and following the path of the pancreas. In the pancreatic body, the splenic vein courses posterior to the gland, and the parenchyma is visualized between the splenic vein and ultrasound transducer. Toward the tail of the pancreas, as the splenic vein courses to the splenic hilum, the vein crosses the pancreatic tail and courses anteriorly.

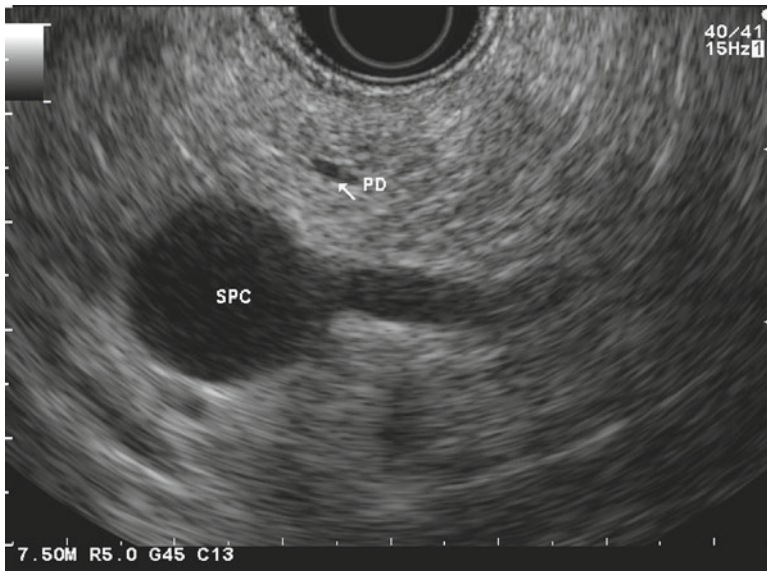


**Fig. 20.** The splenoportal confluence (SPC) represents a critical landmark for identifying the pancreatic body and genu. The SPC has been described as having a “club-like” appearance.

Obviously, the approach to examining the pancreas may vary among experienced endosonographers; however, the anatomical stations and landmarks remain constant. Quick recognition of these landmarks and understanding their anatomical relation to the pancreas will enable the beginner to regain position quickly if disoriented during the exam.

## RECTUM

Rectal endosonography is typically performed to evaluate suspicious polyps, submucosal masses, or stage rectal cancer. Radial EUS can be performed using either a rigid ultrasound probe or standard flexible radial echoendoscope. Rigid probes provide 360° ultrasound imaging similar to standard echoendoscopes. However, rectal probes lack both fiber-optic bundles and charged-couple device (CCD) image sensors, and therefore cannot provide endoscopic images. Due to their rigid nature and lack of endoscopic visualization, rigid probes can only provide sonographic imaging from the rectum and perianal area. Standard, oblique-viewing, flexible radial echoendoscopes can be advanced into the rectum and sigmoid colon under direct endoscopic visualization to provide sonographic imaging from these regions. However, it may be difficult to maneuver the radial echoendoscope beyond the tortuous sigmoid colon due to limited endoscopic visualization and increased risk for perforation.

Patients undergoing EUS of the rectosigmoid colon are typically given an enema or complete bowel preparation to evacuate all stool from the area of interest. The authors prefer a complete bowel preparation as this tends to optimize sonographic imaging and allow endotherapy with electrocautery if necessary. Initially, the patient is placed in the left lateral decubitus position. For the majority of cases, sedation is not necessary but may be preferred depending on the endoscopist and patient preference. Prior to performing the rectal EUS, a flexible sigmoidoscopy is performed to assess the lesion of interest and quality of the bowel preparation. Once the sigmoidoscopy is completed, the radial echoendoscope is gently inserted through the anus and advanced to the sigmoid colon. The balloon is inflated and continuous suction is applied to remove any remaining air within the intestinal lumen. Again, water may be instilled through the biopsy channel to further enhance acoustic coupling. Perpendicular imaging may be difficult in the region of Houston's valves, and therefore, additional water and manipulation of the echoendoscope may be necessary to avoid tangential imaging. From the sigmoid colon, the echoendoscope is slowly withdrawn focusing attention to the intestinal wall and perirectal space.



One of the first landmarks to appear at the level of the distal sigmoid colon is the iliac vessels. The iliac vessels appear as long, tubular, anechoic structures and represent an important landmark for nodal staging in rectal cancer (Fig. 21). Lymph nodes appear as round or oval echogenic structures located in the perirectal space. Usually, lymph nodes can be distinguished from blood vessels by advancing and withdrawing the scope to visualize whether the structure elongates into a long tubular structure suggestive of a vessel or remains fixed like a node. With the development of electronic radial echoendoscopes, the use of Doppler can further aid in discerning nodes from vessels.

When performing rectal endosonography, familiarity with the normal male and female pelvic anatomy is essential. In males, as the echoendoscope is withdrawn from the sigmoid colon into the rectum, the prostate appears as an oval-shaped, hypoechoic, heterogeneous structure located anterior to the rectal wall (Fig. 22). It is not uncommon to observe calcifications within the prostate gland. Once identified, the prostate should be oriented into the 12 o'clock position. With this orientation, the left on the ultrasound image corresponds to the patient's left and right corresponds to the patient's right. Similarly, the top of the image represents the patient's anterior and the bottom represents the patient's posterior. The left and right seminal vesicles are observed just proximal to the prostate and appear as elongated hypoechoic structures located in the 9–12 o'clock and 12 to 3 o'clock positions, respectively. These structures should not be confused with enlarged lymph nodes. In females, the vagina, urethra, uterus, and bladder can also be visualized anterior to the rectum. Similar to the prostate in males, once the uterus is identified, it should be oriented into the 12 o'clock position to obtain proper orientation (Fig. 23).

In the anal canal, the internal and external sphincters are visualized by ultrasound. The internal anal sphincter (IAS) appears as a thin hypoechoic ring surrounding the anal canal. The external anal sphincter (EAS) is seen just lateral to the IAS as a heterogeneous echogenic structure (Fig. 24). In patients with fecal incontinence, trans-anal ultrasound can be useful for evaluating defects in the continuity of the IAS and EAS. Most endosonographers prefer rigid ultrasound probes for optimal evaluation of the anal sphincters.

In addition to suspicious polyps, submucosal masses and rectal cancer, radial EUS can be useful for evaluating perirectal fistulas and abscesses observed in inflammatory conditions such as Crohn's disease (15, 16). Fistulas appear as anechoic or hypoechoic structures within the anorectal region and often demonstrate ultrasound artifact due to air within the fistula. Abscesses may appear as irregularly shaped anechoic or hypoechoic perirectal masses that often have echogenic debris within the

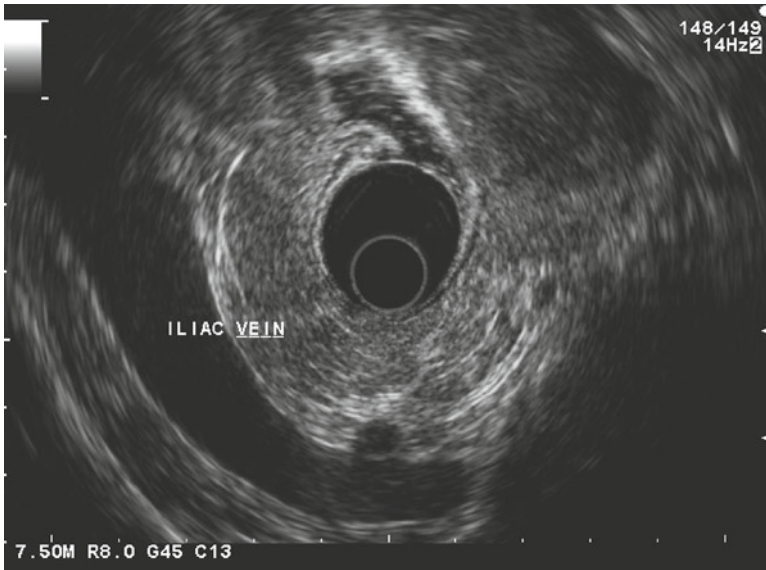


**Fig. 21.** The iliac vessels appear as long, tubular anechoic structure located in the perirectal space near the rectosigmoid junction. The iliac region is important for nodal staging.

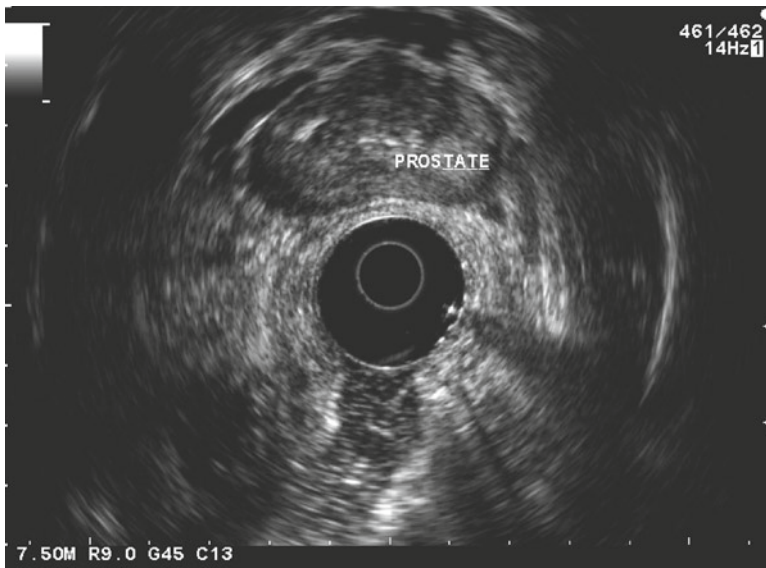


**Fig. 22.** The oval-shaped prostate is hypoechoic and heterogeneous with well-defined borders. It is not uncommon to see calcifications within the gland.

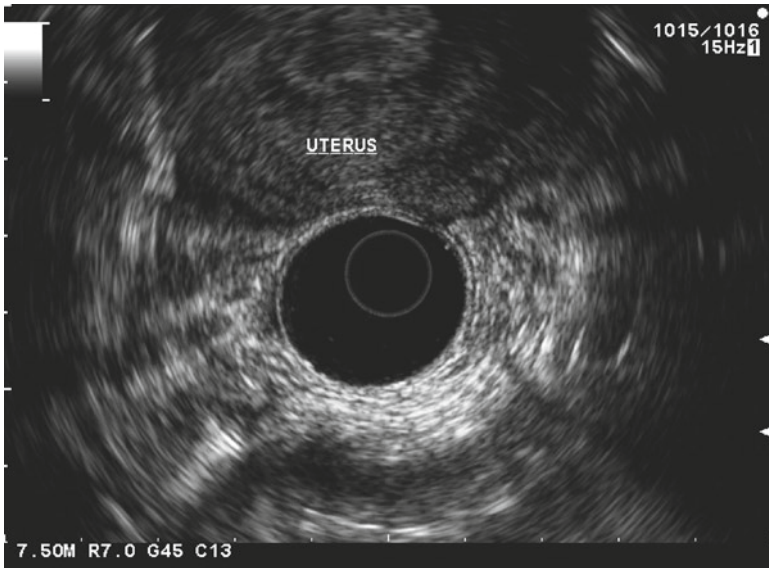


**Fig. 23.** The uterus is a large hypoechoic structure located anterior to the rectal wall. The vagina may be observed between the uterus and rectal wall upon withdrawal of the scope.

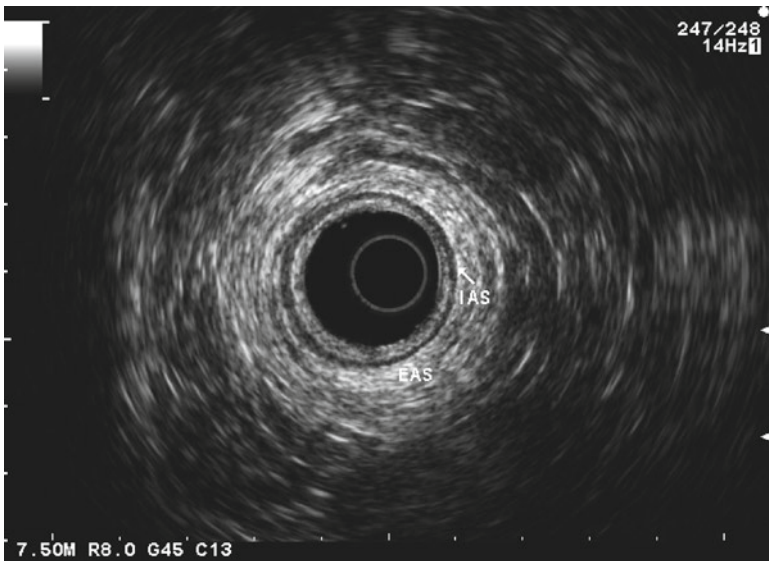


**Fig. 24.** The internal anal sphincter (IAS) is a thin, hypoechoic ring surrounding the anal canal. The external anal sphincter (EAS) is heterogeneous and echogenic and located just lateral to the IAS.

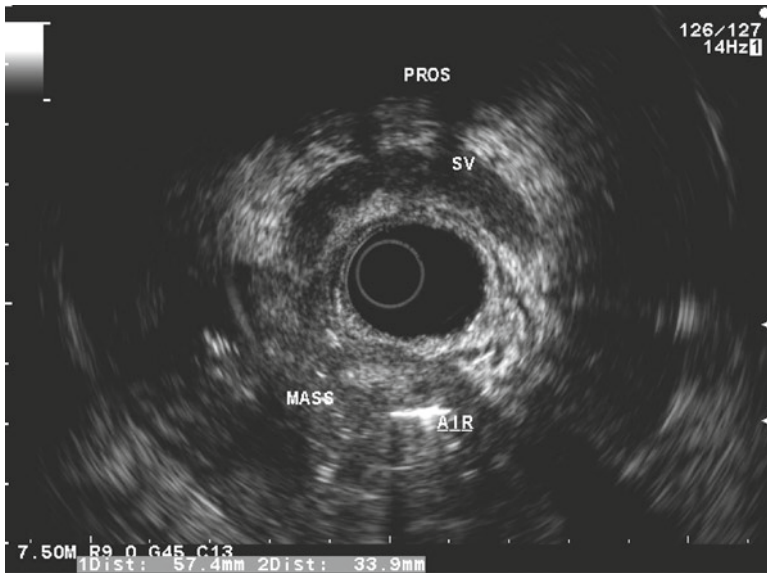


**Fig. 25.** Large presacral abscess demonstrated as complication from prior colorectal surgery. Note the echogenic debris and air within the abscess. The abscess is located posteriorly as depicted by the anterior position of the prostate (PROS) and seminal vesicles (SV).

abscess cavity (Fig. 25). Abscesses may also be seen as complications from prior colorectal surgery.

## SUMMARY

Since its inception over two decades ago, radial EUS has emerged as a powerful diagnostic tool for the evaluation and staging of gastrointestinal neoplasms in both the upper and lower digestive tracts. Although the technology was initially reserved for large, tertiary referral centers, more and more community hospitals are recognizing the increasing demand for EUS, and therefore investing in both equipment and skilled endosonographers. Obviously, reading a textbook chapter or attending a weekend hands-on course is inadequate training for starting an EUS practice. However, textbooks and hands-on courses can serve as excellent adjuncts to dedicated, supervised training. For the beginner, review of an anatomy and radiology atlas is critical for understanding and accurately interpreting the ultrasound images. Acquiring fundamental skills in radial EUS may further assist in learning linear endosonography and

ultimately EUS-guided FNA. Recognizing and remembering the common anatomical landmarks is essential and will ultimately lead to a thorough and efficient exam.

## REFERENCES

1. Verma D, Kapadia A, Eisen GM, et al. EUS vs. MRCP for detection of choledocholithiasis. *Gastrointest Endosc.* 2006;64:248–54.
2. McMahon CJ. The relative roles of magnetic resonance cholangiopancreatography (MRCP) and endoscopic ultrasound in the diagnosis of malignant common bile duct strictures: a critically appraised topic. *Abdom Imaging.* 2008;33:10–3.
3. DeWitt J, Devereaux B, Chriswell M, et al. Comparison of endoscopic ultrasonography and multidetector computed tomography for detecting and staging pancreatic cancer. *Ann Intern Med.* 2004;141:753–63.
4. Liu CL, Lo CM, Chan JK, et al. EUS for detection of occult cholelithiasis in patients with idiopathic pancreatitis. *Gastrointest Endosc.* 2000;51:28–32.
5. Gress F, Bhattacharya I, editors. *Endoscopic ultrasonography.* New Jersey: Wiley-Blackwell; 2001.
6. Hawes RH, Fockens P, editors. *Endosonography.* Philadelphia: Saunders Elsevier; 2006.
7. Bhutani MS, Deutsch JC. *Digital human anatomy and endoscopic ultrasonography.* Ashland (OH): People's Medical Publishing House, USA; 2005.
8. Yusuf TE, Tsutaki S, Wagh MS, et al. The EUS hardware store: state of the art technical review of instruments and equipment. *Gastrointest Endosc.* 2007;66:131–43.
9. Kimmey MB, Martin RW, Haggitt RC, et al. Histologic correlates of gastrointestinal ultrasound images. *Gastroenterology.* 1989;96:433–41.
10. Tio TL, Tytgat GN. Endoscopic ultrasonography of normal and pathologic upper gastrointestinal wall structure. Comparison of studies in vivo and in vitro with histology. *Scand J Gastroenterol Suppl.* 1986;123:27–33.
11. Wiersema M, Wiersema L. High-resolution 25 Megahertz ultrasonography of the gastrointestinal wall: histologic correlates. *Gastrointest Endosc.* 1993;39:499–504.
12. Savides TJ, Gress FG, Zaidi AS, et al. Detection of the embryologic ventral pancreatic parenchyma with endoscopic ultrasound. *Gastrointest Endosc.* 1996;43:14–9.
13. Bhutani MS, Hoffman BJ, Van Velse A. Diagnosis of pancreas divisum by endoscopic ultrasound (EUS). In: 10th International Symposium on Endoscopic Ultrasonography. Cleveland, OH, 1995.
14. Bhutani MS, Hoffman BJ, Hawes RH. Diagnosis of pancreas divisum by endoscopic ultrasonography. *Endoscopy.* 1999;31:167–9.
15. Schratte-Sehn AU, Lochs H, Vogelsang H, et al. Endoscopic ultrasonography versus computed tomography in the differential diagnosis of perianorectal complications in Crohn's disease. *Endoscopy.* 1993;25:582–6.
16. Spradlin NM, Wise PE, Herline AJ, et al. A randomized prospective trial of endoscopic ultrasound to guide combination medical and surgical treatment for Crohn's perianal fistulas. *Am J Gastroenterol.* 2008;103:2527–35.